Numerical and Experimental Static Bending Analysis of Composite Sandwich Panels with Grid-Stiffened Cores Before and After Transverse Impact Loading

Ali Asghar Davoodabadi,
Department of Mechanical Engineering,
Malek Ashtar University of Technology, Tehran, Iran
E-mail: davoodabadi.a@gmail.com, Mohsenheydari1371@gmail.com

Ali Davar *
Faculty of Materials and Manufacturing Processes,
Malek Ashtar University of Technology, Iran
E-mail: a_davar@mut.ac.ir
*Corresponding author

Mohsen Heydari Beni
Department of Mechanical Engineering,
Malek Ashtar University of Technology, Tehran, Iran
E-mail: davoodabadi.a@gmail.com, Mohsenheydari1371@gmail.com

Jafar Eskandari Jam
Composite Research Centre,
Malek Ashtar University of Technology, Tehran, Iran
E-mail: jejaam@gmail.com , eskandari@mut.ac.ir

Received: 29 July 2020, Revised: 19 September 2020, Accepted: 11 November 2020

Abstract: Nowadays grid structures are considered as one of the most useful composites because of their various applications. Since grid structures are vulnerable to impact loads, they should be investigated under such loadings. The present paper studies the low-velocity impact loading of sandwich panels with grid-stiffened cores using both experimental and numerical simulations. In addition to the impact behaviour and the resultant damage of the sandwich panels, the behaviour of these structures under three-point bending was studied before and after the impact loading. The results were provided for impact and bending loadings separately. Then the effect of impact loadings on bending strength was investigated and it was found that the impact loading decreases the bending strength. A consistency between numerical and experimental results was also observed, which confirms the applicability of the Finite Element Method (FEM) in simulating the behaviour of such structures under impact and bending loads, while saving lots of time, efforts and costs.

Keywords: Composite, Finite Element Method, Grid Structures, Sandwich Panels

How to cite this paper: Ali Asghar Davoodabadi, Ali Davar, Mohsen Heydari Beni, and Jafar Eskandari Jam, "Numerical and Experimental Static Bending Analysis of Composite Sandwich Panels with Grid-Stiffened Cores Before and After Transverse Impact Loading", Int J of Advanced Design and Manufacturing Technology, Vol. 15/No. 1, 2022, pp. 1–9. DOI: 10.30495/admt.2021.1904974.1208

Biographical notes: Ali Asghar Davoodabadi received his MSc in Mechanical Engineering from University of Malek Ashtar, Iran, in 2016. His field of research is mechanical analysis of composite materaials. **Ali Davar** is currently Associate Professor at the Department of Mechanical Engineering, at Malek Ashtar University, Tehran, Iran. He received his PhD in Mechanical Engineering from Khajeh Nasir Toosi University, Iran, in 2010. **Mohsen Heydari Beni**, is currently a PhD student at Malek Ashtar University. He received his MSc in Mechanical Engineering from Shahrekord University, Iran, in 2015. **Jafar Eskandari Jam** is Professor of Mechanical Engineering at Malek Ashtar University Tehran, Iran. He received his PhD in Mechanical Engineering from Anna State University, India, in 2000. His current research focuses on composite structures, plates and shell analysis and nanomechanics.

1 INTRODUCTION

Grid structures are one of the most advanced and novel patterns employed in the design of composite structures. However, these configurations have a long history of application in structures composed of isotropic materials, such as metal structures. The use of composites in grid structures provides the opportunity to utilize the longitudinal properties (in the fiber direction) of the composites in different directions of the structure. Recently, lots of research have been directed towards the optimization of patterns to increase the distribution of the mechanical properties of the composites within the structure. Among the Polymer Matrix Composites (PMCs), the design and use of continuous fiber reinforced polymers are the most complicated, since they should be employed in a way that the highest structural strength is obtained in the direction subjected to the largest loads [1].

Recently, these types of composites have been occasionally used in the construction of grid structures. This combination leads to a structure with the lowest possible weight. Composite grids are constructed such that the fibers are arranged along the grid lines, known as the ribs, which utilize the highest possible strength of composite layers. This condition along with the proper engineering characteristics, such as high stiffness, high strength to weight ratios, high energy absorption, efficient thermal insulation and sandwich panels' capabilities, has made the composite grids as one of the most widely used structures. Kidan et al. [2-3] studied the buckling behavior of the grid structures under axial loads. The affectability of buckling critical load due to the variation of different parameters was also investigated. The equivalent shell's buckling load was calculated by using the modified equalization method and minimization of the total potential energy.

Gan and Gibson [4] investigated the energy absorption of a composite grid structure under transverse loading by analytical solutions and experimental tests. They constructed a composite grid panel with a shell side and tested it by placing the panel on a three-point bending test fixture on both sides. Fan et al. [5] investigated the behavior of sandwich panels stiffened with hexagonal carbon fiber arrangement. The experimental results indicated that the carbon reinforced grid structure was stiffer and stronger than the honeycomb foams. Ribs were required at least in three directions to achieve the necessary shear strength for the grid structure. Thus, a hexagonal grid structure was found to be an optimal choice. Zhang et al. [6] developed a progressive failure analysis method to simulate the start and propagation of the multiple failure modes for composite grid panels and shells based on the stiffness element model. Arashmehr et al. [7] studied sandwich panels with grid-stiffened cores under tensile loading both analytically and experimentally. Results showed that the intersection of the ribs plays an important role in reducing the von-mises stress. It was also found that the shells reinforced with inclined ribs significantly increase the load bearing capacity of the structure. Petras [8] investigated the sandwich beams made of laminated Glass Fiber Reinforced Plastic (GFRP) skins enclosing Nomex honeycomb core. Experimental tests and analytical solutions were carried out and the failure map was established in terms of the ratio of skin thickness to the span length.

Triantafillou et al. [9] applied the similar approach for establishing the failure mode maps for foam core sandwich beams by quantifying the peak load through a three point bending test. Following these, analytical models were established to predict the elastic behavior and bending strength of sandwich panels [10-11]. Hozhabr et al. [12-13] studied the in-plane compression responses of an aluminum honeycombs filled with foams. It was found that the bearing capacities of this structure are higher than the single honeycombs'. Thomas et al [14] studied the residual strength of impact-damaged sandwich, which is caused by low-energy impacts like hail and bird strikes, by numerical modeling. Mamalis et al [15] investigated the in-plane compression properties, collapse modes and crushing characteristics of composite sandwich panels with different core materials and fiber reinforced skins.

2 METHODOLOGY

2.1. The Construction Method, Raw Materials, and Construction Process

Glass fibers and epoxy resin were employed to construct the sandwich panels. The panels' cores were composed of K28-084 glass fibers saturated with thermoset epoxy resin [6]. Unidirectional glass fibers saturated with thermoplastic epoxy resin were used to construct the shells on both sides of the sandwich panel. A silicon frame was provided to construct the grid-stiffened core. The grid structure of the core was manually built by the wet lay-up technique. For this purpose, once the fixture and silicon frame were prepared, the manual twisting process was initiated from end of the first rib on one side and prorogated to the aligned layers. It should be noted that the fibers used in this process were completely pre-impregnated with resin in the epoxy bath. Once the lay-up process of the grid-stiffened core was completed, the structure and fixture were subjected to a curing cycle in an autoclave to be cured for 2 and 3 hours at 80°C and 140°C, respectively.

2.2. Experimental Bending Test Stages

As shown in "Fig. 1", a Zwick/z050 machine with capacity of five tons and an automatic pneumatic jaw was utilized for the three-point bending test. The

displacement rate was set to 1 mm/s. The three-point bending test fixture and its components are illustrated in "Fig. 2".

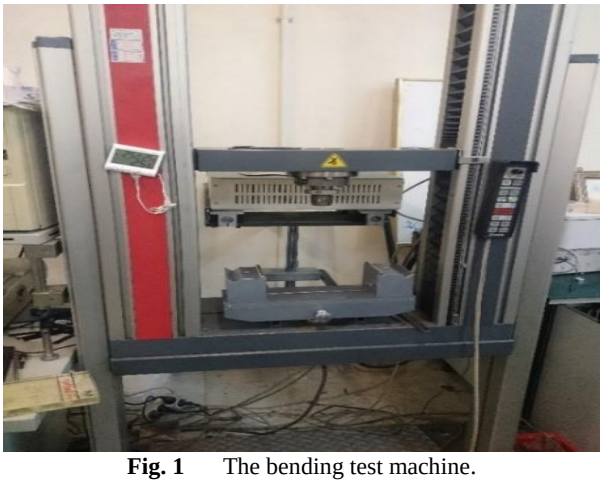

Fig. 1 The bending test machine.

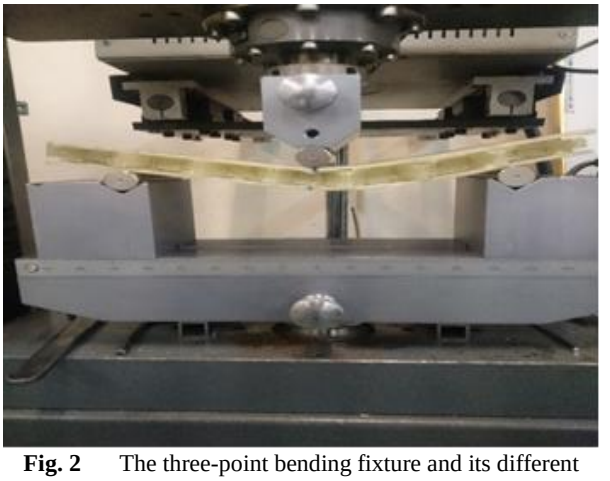

Fig. 2 The three-point bending fixture and its different components.

For the sake of quasi-static condition, the moving jaw of the machine was set to apply the bending load to the panel at the speed of 1 mm/min. The distance between the two bars at the bottom was 205.65 mm, with the top bar resting between these bars. The diameter of the fixture bars was 1 cm. The mentioned impact test stages were applied to the first specimen. The part of the shell subjected to the impact (i.e., the middle of the specimen) was placed in the bottom section, while the jaw was placed above the specimen. The results are provided in details in section 5.

3 NUMERICAL MODELING

This section studies the low-velocity impact loading of a glass-epoxy composite sandwich panel with a grid-stiffened core by the numerical simulation software, ABAQUS. The sandwich panel dimensions were 303*100*21 mm and it was composed of two components; a grid part and the ribs. The shells on both sides had a 3 mm thickness and the grid-stiffened core accounted for 15 mm of the sandwich panel's thickness. In order to investigate the impact responses of the structure, an object was dropped on the composite panel from the height of 50 cm.

The impacting object's weight was 11.32 kg, with an effective spherical impact diameter of 16 mm. The entire core was modeled as an integrated object while the impacting object was modeled as a semi-spherical rigid body with a diameter of 16 mm, to reduce the computational time. The model was actually the end part of a punch. The three dimensional (3D) elements were applied to discretize the sandwich panel. The broom meshing method with hexagonal elements was employed on the ribs, while structured hexagonal elements were used to mesh the shells of both sides. The entire elements were 3D and they are known as C3D8R elements in ABAQUS.

3.1. Material Properties and Lay-Up

It is really important to determine the materials of composite structures, since despite of metals, both the materials and the lay-up significantly affect the results [3]. Table 1 provides the mechanical properties of the sandwich panel's shells, while "Table 2" shows the mechanical properties of the ribs.

Table 1 The mechanical properties of the two sides of the sandwich panel's shells [13]

Elastic Properties		Strength	
E_1(GPa)	17.8	X_t(MPa)	450
E_2/E_3 (GPa)	4.2	X_c(MPa)	283
$\upsilon_{12}/\upsilon_{13}$	0.275	Y_t(MPa)	24
υ_{23}	0.38	Y_c(MPa)	80
G_{12}/G_{13} (GPa)	3.6	S_L(MPa)	21
G_{23} (GPa)	2.2	S_T(MPa)	21

Table 2 The mechanical properties of the ribs [3]

Elastic Properties		Strength	
E_1(GPa)	22.5	X_t(MPa)	514
E_2/E_3 (GPa)	7.63	X_c(MPa)	300
$\upsilon_{12}/\upsilon_{13}$	0.22	Y_t(MPa)	81.7
υ_{23}	0.29	Y_c(MPa)	197
G_{12}/G_{13} (GPa)	2.37	S_L(MPa)	69
G_{23} (GPa)	3.13	S_T(MPa)	69

3.2. The Study of Mesh Convergence

Figure 3 plots the maximum contact load of impacts versus the number of elements. The optimized number of elements is the starting point of the horizontal line.

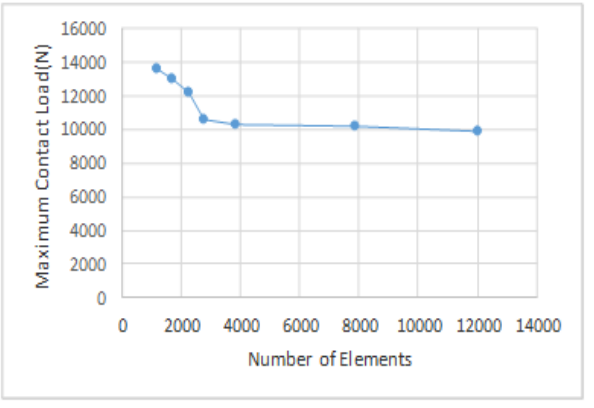

Fig. 3 Mesh convergence for the impact test.

4 RESULTS AND DISCUSSION

The impact is applied to the middle of the rib (intersection) at the center of the sandwich panel. Figure 4 compares the impact locations of the sandwich panel in the numerical and experimental models and "Fig. 5" shows the impact location on the center to provide a better visualization.

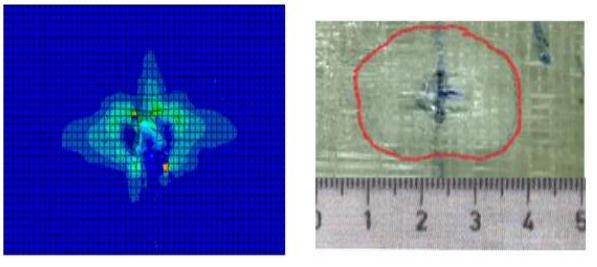

Fig. 4 Comparing the numerical and experimental impact locations of the sandwich panel.

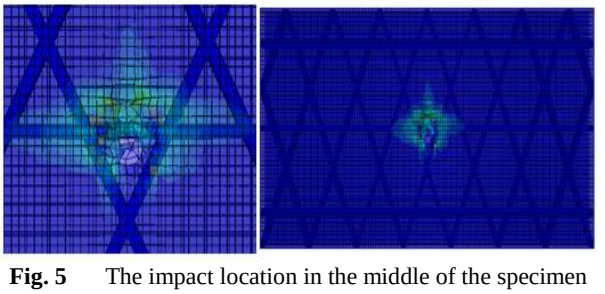

Fig. 5 The impact location in the middle of the specimen on the rib.

Figure 6 plots the contact load, between the sandwich panel and the impacting object, in the middle of the panel versus time for both the experimental and numerical results. The collision time and the maximum contact load are important in the investigation of the impact responses. According to "Fig. 6", the numerical and experimental results for the collision time are in good agreement. Also, the numerical contact load is reasonably consistent with the experimental results. The maximum numerical and experimental contact loads were found to be 10 and 12 KN, respectively. This difference could be attributed to the factors such as, small geometric differences between the experimental and numerical models, small differences in the material properties, or the defects within the experimental specimen. Figure 7 represents the kinetic energy of the impacting objects diagram during its collision with the sandwich panel.

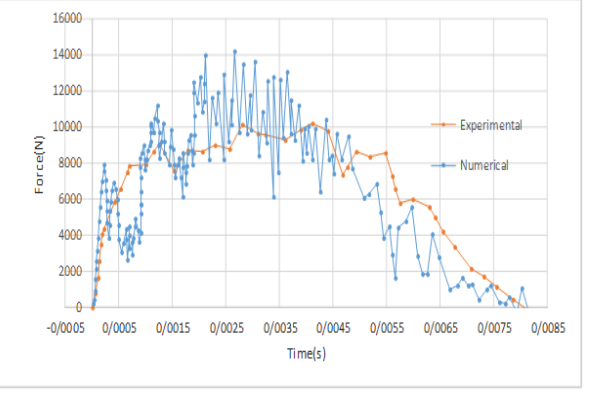

Fig. 6 The experimental and numerical plots of impact acceleration on the sandwich panel.

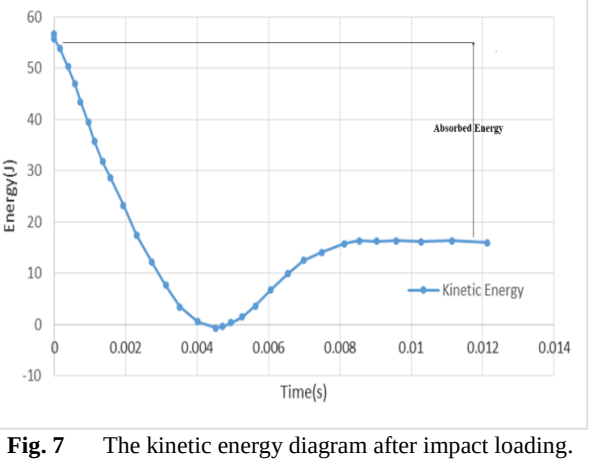

Fig. 7 The kinetic energy diagram after impact loading.

Based on the modeling performed to find the energy level that causes an observable energy in the specimen, 44 J of energy was selected to be applied as the impact load. According to "Fig. 7", the 55J kinetic energy in the beginning of collision decreased to 17 J at the end of collision. Thus, the absorbed energy of the sandwich panel was calculated to be 38 J, according to the numerical results. The remaining energy was consumed to propagate elastic waves. As can be seen, the structure damage and deformation absorbed the induced energy of the impact. The initial energy of the impacting object is

transformed to the structure while colliding with the sandwich panel, which damages the composite. The remaining energy is transformed into elastic energy.

5 FINITE ELEMENT ANALYSIS AND THREE-POINT BENDING EXPERIMENT OF THE GRID PANEL BEFORE IMPACT LOADING

Given that the three-point bending test is a quasi-static one, the dynamic explicit solver of ABAQUS was employed with a step increment of 0.1. Also, the panel's shape was considered to be nonlinear. A large change or displacement in the three-point bending test is another reason for the use of the dynamic explicit solver. The contact between the bar and panel was defined as a general contact interaction that allows for defining the interactions between several or all the sections of a model by only one interaction. The contact was considered as a penalty contact in the tangent direction with a friction coefficient of 0.5 and as a hard contact in the vertical direction, i.e., the bar and panel did not penetrate each other. A reference point and a specific mass were applied to each rigid bar. The applied meshing tools were the same as the ones used in the section 4, with the difference that S3D4 elements were used to model the bending enforcer rigid bar as shown in "Fig. 8".

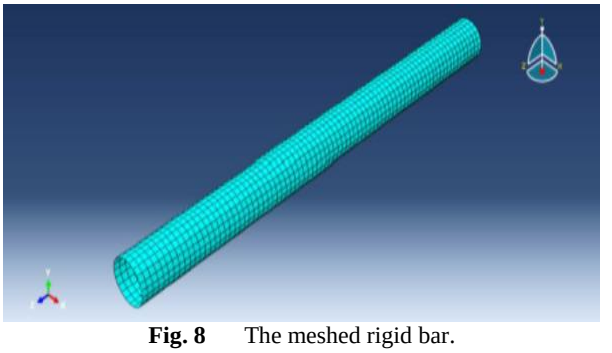

Fig. 8 The meshed rigid bar.

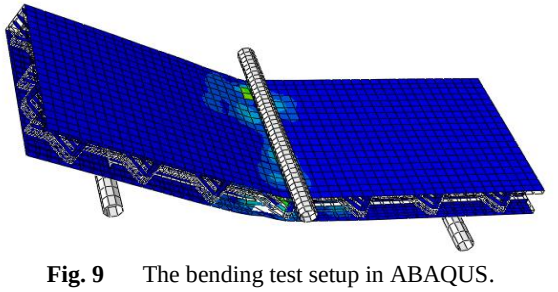

Fig. 9 The bending test setup in ABAQUS.

5.1. The Three-Point Bending Test Results Before the Impact Loading

Figures 9 and 10 depict the three-point bending setup in ABAQUS along with the experimental one. Figure 10 shows the non-impact loaded specimen before and during the bending. Figure 11 illustrates the kinetic and internal energy of the analyzed model.

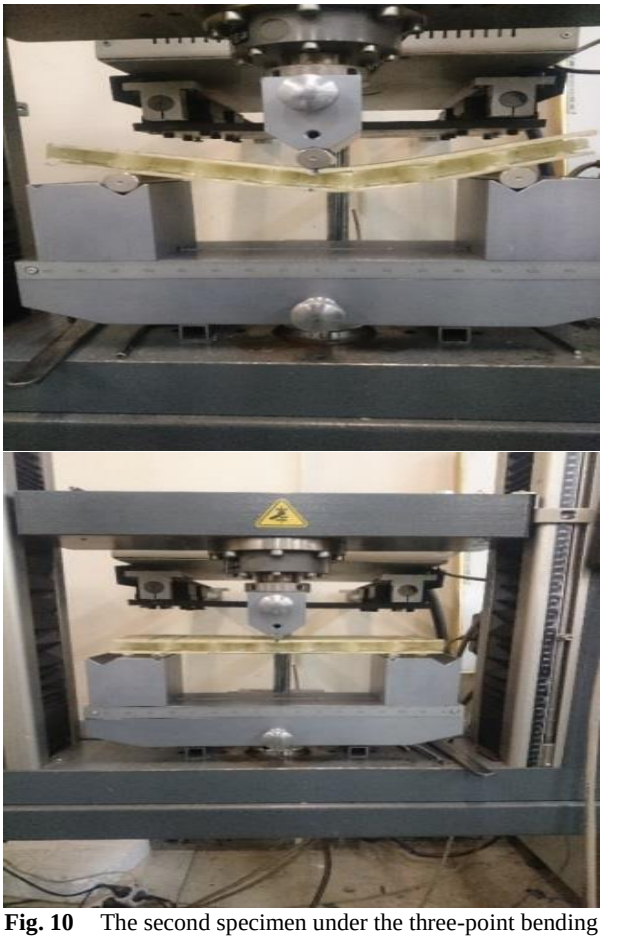

Fig. 10 The second specimen under the three-point bending load.

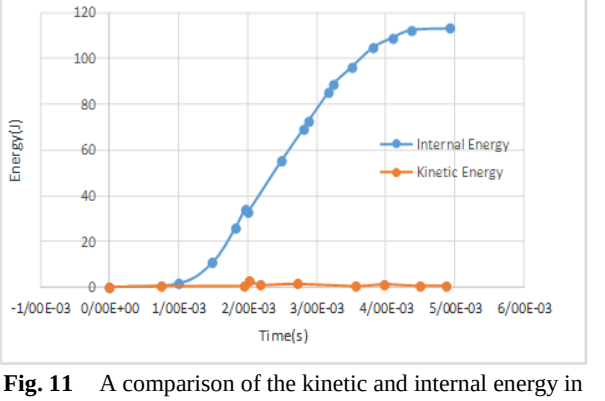

Fig. 11 A comparison of the kinetic and internal energy in bending analysis.

Furthermore, "Fig. 12" compares the experimental and numerical load-displacement curves for the non-impact loaded model. As can be seen, the first failure for the experimental and numerical models occurred at 3.9 and 4.9 mm of displacement, respectively, after which the

structure continued to absorb energy. Then, after the local separation of the shell and layers at point B, the specimen underwent failure in the core by re-absorbing energy.

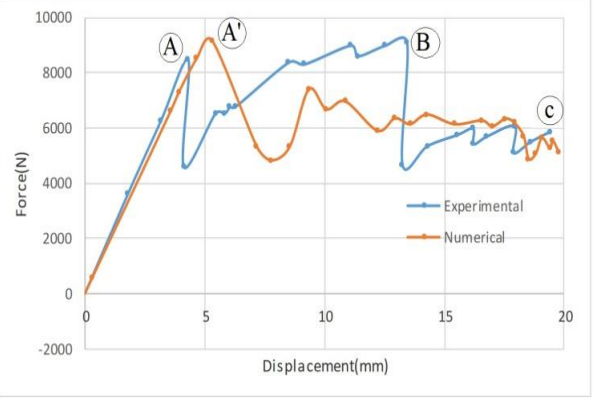

Fig. 12 A comparison of the numerical and experimental results of the non-impact loaded specimen under the bending load.

According to the numerical results, the composite structure absorbed 119.29 J of energy until 20 mm of displacement. However, this parameter for the experimental model was 128 J. The difference of nearly 9 J could be caused by construction defects. The investigation of the area under the load-displacement curve indicates that the energy of the first failure was 25 J and 15.8 J for the numerical and experimental models, respectively. The difference between these results can be attributed to the previously mentioned reason and also to the exclusion of plate separation in the numerical model.

6 INVESTIGATING FAILURE MODES IN THE EXPERIMENTAL MODEL

The maximum load that the structure underwent was considered as the failure criterion. Given the high energy absorption of the structure after failure, no rapid decline was seen in the load-displacement diagram. Thus, this phenomenon in the experimental diagram is due to the inter-layer separation, which was observed during the test. Also, failure modes were observed between the fibers, causing local reductions in the experimental diagram. Since fibers are more brittle than the matrix they cannot be as stretched as the matrix. Thus, they are weak in terms of strain, and the excreted strain in this test causes the fibers to rupture.

6.1. The Finite Element Analysis of Three-Point Bending of the Grid Panel After the Impact Loading

As shown in "Fig. 13" in the first stage the specimen underwent an impact loading with the same conditions mentioned in section 3. Then, the same specimen underwent a three-point bending load as shown in "Fig. 14".

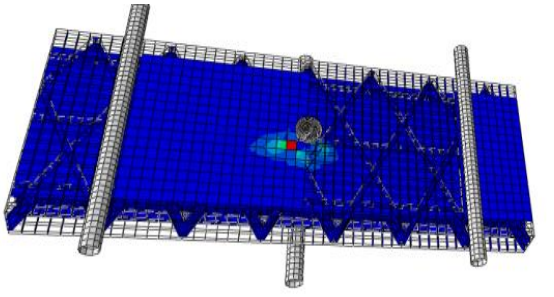

Fig. 13 The numerical modeling of the impact stage.

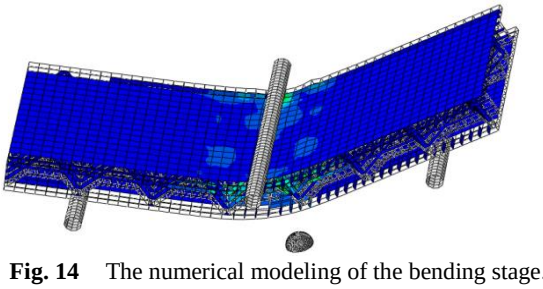

Fig. 14 The numerical modeling of the bending stage.

7 RESULTS OF BENDING AFTER THE IMPACT LOADING

Figure 15 compares the numerical and experimental results of bending after the impact loading.

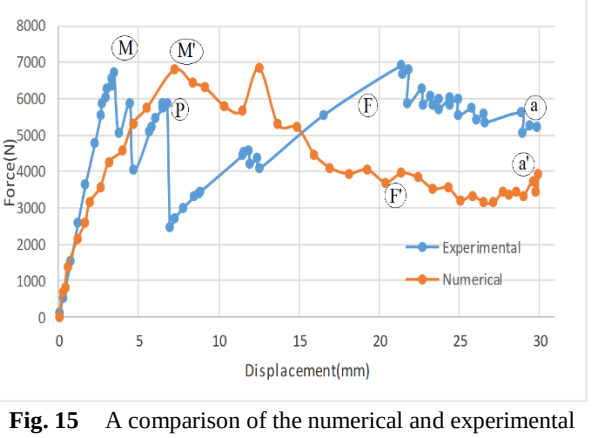

Fig. 15 A comparison of the numerical and experimental results after impact loading.

In the experimental model, the first failure occurred at approximately 4 mm (3.7 mm) of displacement along with breakage sound. The structure continued to absorb energy until a rapid decline in the load occurred at point P, and the local separation of the shell from the core took place. Then, the core continued to absorb energy for 20 more times, with the load fluctuating due to the local failures. Finally, after some local failures in the core, the

structure underwent the ultimate failure due to the core destruction. The first failure for the numerical results occurred at approximately 7 mm of displacement.
Furthermore, for the experimental model the energy absorptions for 20 mm of displacement and the first failure were obtained to be nearly 94 J and 28 J, respectively. However, for the numerical simulations these parameters were found to be 86 J and 12 J, respectively. The difference between the numerical and the experimental results can be attributed to construction defects and also to the exclusion of plate separation in the numerical model. Table 3 reports the difference between the experimental and numerical models before local shell separation at point P. Also, "Table 4" shows the displacements of failure points in the impact-loaded bending test.

Table 3 The energy absorption of the bending test with the impact loading

Energy	Numerical Model	Experimental Model
First failure point (M)	28 J	12.3 J
Shell separation point (P)	25 J	28 J
Ultimate point(Q) at 30mm	130.42 J	145 J

Table 4 The displacements of the failure points in the impact-loaded bending test

Displacement	Numerical Model	Experimental Model
First failure point (A)	7 mm	3.7 mm

8 INVESTIGATION OF THE IMPACT DAMAGE

In this section the variation of bending strength due to the impact load prior the bending is investigated separately for the experimental and the numerical results.

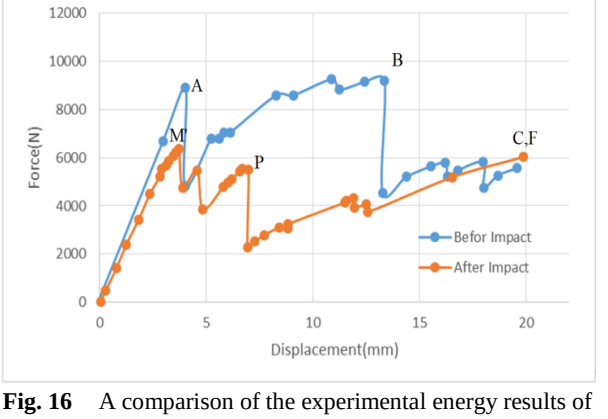

Fig. 16 A comparison of the experimental energy results of an impact-loaded specimen and a non-impact loaded specimen.

8.1. Investigation of the Impact Damage in The Experimental Bending Test

Figure 16 illustrates the experimental bending test results for two specimens, one before and the other one after the impact. As can be seen, the first failure occurred at almost the same displacement (approximately 4 mm) for both specimens. However, the damage induced by the impact with the energy of 38 J was transformed into internal energy and considerably reduced the load required for the first failure. Table 5 represents the experimental energy results of the two specimens, ("Table 6").

Table 5 A comparison of experimental energy results of the two specimens

Energy	Experimental Impact-loaded Model	Experimental Non-impact Loaded Model	Variation Percentage
First failure point (M, A)	12.3 J	15.8 J	22
Shell separation point (P) at 7 mm	28 J	34 J	17
Ultimate test point (C,F) at 20 mm	86.7 J	128 J	32

Table 6 The displacement of failure points in the bending test

Displacement	Impact-loaded Experimental Model	Non-impact Loaded Experimental Model
First failure point (A)	3.7 mm	3.9 mm

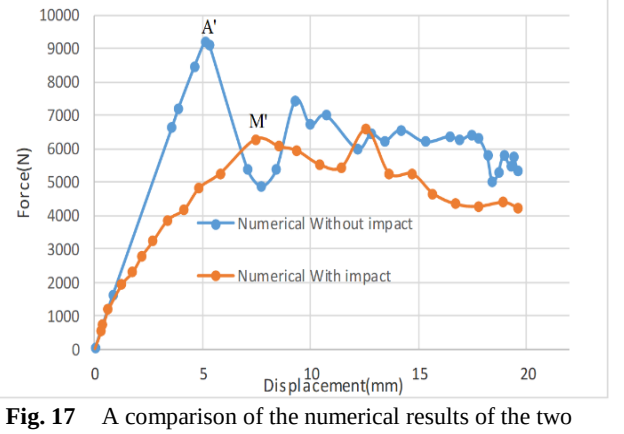

Fig. 17 A comparison of the numerical results of the two specimens.

9 INVESTIGATING THE IMPACT DAMAGE IN THE NUMERICAL BENDING TEST

Figure 17 compares the numerical results of the impact-loaded and non-impact loaded specimens. Also, "Table 7" represents the numerical results that were discussed in the previous sections. As can be seen, the damage induced by the impact load dramatically decreased the energy absorption of the bending-subjected specimen.

Table 7 A comparison of the numerical energy absorption results

Energy	Impact-loaded Numerical Model	Non-impact Loaded Numerical Model
Ultimate point (20 mm)	94.72 J	119.29 J

10 CONCLUSION

In this study, the low-velocity impact loading and three-point bending tests were carried out on a sandwich panel with a grid-stiffened core. The effect of impact loading on the bending strength of the specimen was also investigated. The numerical simulations and experimental tests yielded the following results:

1- For impact-loaded composite structures, a portion of the initial energy is consumed to propagate elastic waves in the structure and to damage the structure, while the remaining energy is consumed by the impacting object to bounce again. In the present study, approximately 30% of the energy was consumed by impacting object, while the remaining energy was maintained in the specimens in the form of damage.

2- The impact damage considerably reduced bending strength. It varied between 17-32% in the present work, depending on the test conditions.

3- For a composite grid panel under quasi-static loading, failure modes typically include; the failure due to the longitudinal tension in the underlying layers, the buckling and micro-buckling of fibers in upper layers under compressive tension and the transverse shear near the boundary conditions. Tensile and transverse shear modes were observed along with layer separation.

REFERENCES

[1] Winson, J. R., Mechanics of Composites, Publications of Amirkabir University of Technology, 2003.

[2] Kidane, S., Buckling Analysis of Grid Stiffened Composite Structures, Faculty of the Louisiana State University and Agricultural and Mechanical College in Partial Fulfillment of the Requirements for The Degree of Master of Science in Mechanical Engineering in The Department of Mechanical Engineering by Samuel Kidane B. Sc., Addis Ababa University, 2002.

[3] Kidane, S., Li, G., Helms, J., Pang, S. S., and Woldesenbet, E., Buckling Load Analysis of Grid Stiffened Composite Cylinders, Composites Part B: Engineering, Vol. 34, 2003, pp. 1-9.

[4] Gan, C., Gibson, R. F., and Newaz, G. M., Analytical/Experimental Investigation of Energy Absorption in Grid-Stiffened Composite Structures Under Transverse Loading, Experimental Mechanics, Vol. 44, 2004, pp. 185-194.

[5] Fan, H., Meng, F., and Yang, W., Sandwich Panels with Kagome Lattice Cores Reinforced by Carbon Fibers, Composite structures, Vol. 81, 2007, pp. 533-539.

[6] Zhang, Z., Chen, H., and Ye, L., Progressive Failure Analysis for Advanced Grid Stiffened Composite Plates/Shells, Composite Structures, Vol. 86, 2008, pp. 45-54.

[7] Arashmehr, J., Rahimi, G. H., and Rasouli, S. F., An Experimental and Numerical Investigation of a Grid Composite Cylindrical Shell Subjected to Transverse Loading, Strojniški Vestnik-Journal of Mechanical Engineering, Vol. 59, 2013, pp. 755-762.

[8] Petras, A., Sutcliffe, M., Failure Mode Maps for Honeycomb Sandwich Panels, Composite Structures, Vol. 44, 1999, pp. 237-52.

[9] Triantafillou, T. C., Gibson, L. J., Failure Mode Maps for Foam Core Sandwich Beams, Materials Science and Engineering, Vol. 95, 1987, pp. 37-53.

[10] McCormack, T., Miller, R., Kesler, O., and Gibson, L., Failure of Sandwich Beams with Metallic Foam Cores, International Journal of Solids and Structures, Vol. 38, 2001, pp. 4901-20.

[11] Banghai, J., Zhibin, L., and Fangyun, L., Failure Mechanism of Sandwich Beams Subjected to Three-Point Bending, Composite Structures, Vol. 133, 2015, pp. 739-45.

[12] Mozafari, H., Molatefi, H., Crupi, V., Epasto, G., and Guglielmino, E., In Plane Compressive Response and Crushing of Foam Filled Aluminum Honeycombs, Journal of Composite Materials, Vol. 49, 2015, pp. 3215-28.

[13] Mozafari, H., Khatami, S., Molatefi, H., Crupi, V., Epasto, G., and Guglielmino, E., Finite Element Analysis of Foam-Filled Honeycomb Structures Under Impact Loading and Crashworthiness Design, International Journal of Crashworthiness, Vol. 21, 2016, pp. 148-60.

[14] Lacy, T. E., Hwang, Y., Numerical Modeling of Impact-Damaged Sandwich Composites Subjected to Compression-After-Impact Loading. Composite Structures, Vol. 61, 2003, pp. 115.

[15] Mamalis, A., Manolakos, D., Ioannidis, M., and Papapostolou, D., On the Experimental Investigation of Crash Energy Absorption in Laminate Splaying Collapse Mode of FRP Tubular Components. Composite Structures, Vol. 70, 2005, pp. 413-29.